Journal of Plant Biology (2022) 65:291–310
https://doi.org/10.1007/s12374-021-09321-6

RESEARCH ARTICLE

Comparative Analysis of miRNA Expression Profiles Provides Insight into Regulation of Biosynthesis of Flavonoids and Terpenoids Between Two Varieties of *Toona sinensis* Sprouts

Hu Zhao[1,2] · Xiaopu Shi[1] · Cheng Shen[1] · Caifeng Chen[1,2] · Changqing Qu[1,2] · Gopal Patel[3] · Wei Zhou[3] · Guoyin Kai[3]

Received: 10 December 2020 / Revised: 20 April 2021 / Accepted: 23 May 2021 / Published online: 7 June 2021

Abstract

In this study, small RNA sequencing has been performed to identify the miRNAs and explore their regulatory mechanism in *T. sinensis* sprouts. From HPLC analysis, the flavonoid content was higher in the BYC2 (purple toon sprout) than in the GYC2 (green toon sprout), whereas the volatile terpenoids revealed an inverse change. Therefore, the small RNA libraries of two varieties were constructed, and 331 known miRNAs and 23 novel miRNAs were discovered. Differential gene expression analysis demonstrated the upregulation of 25 miRNAs and the downregulation of 27 miRNAs between BYC2 and GYC2. qRT-PCR analysis showed that nine miRNAs involved in the biosynthetic regulation of flavonoids were downregulated in the BYC2, whereas eight miRNAs related to the regulation of the biosynthesis of terpenoids were upregulated, when compared with GYC2. The results indicated that the differential expression of the miRNAs mentioned above played a crucial role in the regulation of the formation of the flavonoids and terpenoids in *T. sinensis* sprouts. The present study not only fills in the paucity of knowledge regarding the *T. sinensis* miRNA, it also provides more valuable information for the genetic improvement of *T. sinensis* cultivation for the future.

Keywords Flavonoids · Terpenoids · miRNA · *T. sinensis* · High-throughput sequencing · Post-transcriptional regulation

Abbreviations

AACT	Acetyl-CoA-acetyltransferase
ARF	Auxin response factor
BYC2	Black Youchun
CHS	Chalcone synthase
C4H	Cinnamic acid 4-hydroxylase
4CL	4-Coumarate CoA ligase
DFR	Dihydroflavonol 4- reductase
DXS	1-Deoxy-D-xylulose-5-phosphate synthase
ERF	Ethylene-responsive transcription factor
FAS	(*E*)-β-farnesene synthase
F3H	Flavanone 3-hydroxylase
FLS	Flavonol synthase
FPPS	Farnesyl diphosphate synthase
GDS	(-)-Germacrene D synthase
GO	Enrichment Gene Ontology enrichment
GYC2	Green Youchun
MBW	MYB-bHLH-WD40 (MBW) transcription complex
miRNA	MicroRNA
MEP	2-*C*-methyl-D-erythritol-4-phosphate
MYB	Myeloblastosis
HMGR	3-Hydroxy-3-methyl glutaryl coenzyme A reductase
HCT	Shikimate *O*-hydroxycinnamoyltransferase
HDS	4-Hydroxy-3-methylbut-2-enyl-diphosphate synthase
KEGG	Pathway kyoto encyclopedia of genes and genomes pathway
LAR	Leucoanthocyanidin reductase
KS	Ent-kaur-16-ene synthase
LDOX	Leucoanthocyanidin dioxygenase
LIS	Linalool synthase
LS	(*R*)-limonene synthase
MK	Mevalonate kinase

✉ Hu Zhao
zhaohu8196@sina.com

[1] Biology and Food Engineering College, Fuyang Normal University, Fuyang 236037, Anhui, China

[2] Engineering Technology Research Center of Anti-Aging Chinese Herb, Fuyang Normal University, Fuyang 236037, Anhui, China

[3] Laboratory of Medicinal Plant Biotechnology, Pharmacy College, Zhejiang Chinese Medicine University, Hangzhou 311402, Zhejiang, China

PAL	Phenylalanine ammonia lyase
PMK	Phosphomevalonate kinase
qRT-PCR	Quantitative real-time PCR
SE	Squalene epoxidase
SQS	Squalene synthase
sRNA	Small RNA
SPL	Squamosa promoter-binding protein-like
TPS	Terpene synthases
UGT	Anthocyanidin 3-*O*-glucosyltransferase
WRKY	WRKY transcription factor
ZIP	Homeodomain leucine zipper

Introduction

Toona sinensis (A. Juss) Roem, commonly called the Chinese toon, is a deciduous tree of Meliaceae and is widely distributed across Asia, including China, India, and North Korea (Edmonds and Staniforth 1998). The sprouts or the young shoots of the plant are very popular in vegetarian cuisine for their unique flavor and high nutrition (Zhai and Granvogl 2019). The consumption of toon sprouts as raw material, as toon tea or toon beef sauce is favored by consumers all over the world (Zhao et al. 2019). The seeds, roots, bark, and leaves too, have been well known over a long time for their oriental medicinal properties (Chen et al. 2019). These characteristics in *T. sinensis* are induced by the presence of a large number of natural active compounds, such as polyphenols, flavonoids and terpenoids, etc. (Shen et al. 2017; Peng et al. 2019). Besides the nutritional value, the high concentration of secondary metabolites present in the toon sprouts showed the beneficial effects on human health, which increased the interest of the researchers to discover the details regarding the secondary metabolic pathways.

Since *T. sinensis* is a non-model plant and its genomic background still remains unknown, many of the reports available at present dealing with the secondary metabolic pathways of *T. sinensis* were based on the transcriptome sequencing analysis (Zhang et al. 2016; Sui et al. 2019; Zhao et al. 2019). In our earlier study, some dominant genes involved in the biosynthetic pathways of the flavonoids were identified in the toon bud transcriptome and the anthocyanin contents were comparatively analyzed between the purple toon (Black Youchun: BYC2) and green toon (Green Youchun: GYC2) (Zhao et al. 2017). Many putative unigenes, related to the terpenoids metabolism were also examined in the postharvest toon buds after cold storage (Zhao et al. 2019). Two terpene synthase genes related to the terpenoids biosynthesis were isolated and functionally characterized (Hsu et al. 2012). Liu et al. (2019) have accomplished the sequencing of the complete chloroplast genome of *T. sinensis* using the Illumina sequencing platform. Apart from these reports, no other molecular information is available on the biosynthesis and regulation of the secondary metabolites in *T. sinensis*.

To a large degree, plant development and the biosynthesis of its secondary metabolites are regulated by the microRNAs (miRNAs) and their targets, encoding the functional genes or transcription factors (Samad et al. 2017). As post-transcriptional regulators, the miRNAs are an endogenous group of non-coding small molecular single RNA strands, 20–24 nucleotides (nt) in length (Bulgakov and Avramenko. 2015; Singh et al. 2018Zhang et al. 2018). In plants, the miRNAs reveal high diversity and conservative properties across species, with one of their distinct features being the hairpin structure in their precursors. The plant miRNAs show high complementarity to target the transcripts through base pairing and mediate endogenous specific messenger RNA (mRNA) cleavage or translation repression at the post-transcriptional level, which results in silencing the target gene (Rogers and Chen 2013). In general, the miRNAs are a class of key regulators of physiological processes in plants.

The involvement of the miRNAs in the post-transcriptional regulation of the biosynthesis of the secondary metabolites in medicinal plants has been reported in *Salvia miltiorrhiza*, *Catharanthus roseus*, *Picrorhiza kurroa*, *Xanthium strumarium*, and *Rauvolfia serpentina* (Fan et al. 2015; Prakash et al. 2015, 2016; Vashisht et al. 2015; Xu et al. 2015). Many genes related to the flavonoid biosynthesis were targeted by the miRNAs, like phenylalanine ammonia lyase (*PAL*), dihydroflavonol 4-reductase (*DFR*), 4-coumarate CoA ligase (*4CL*), chalcone synthase (*CHS*) targeted by the miR1873, miR172i, and miR829.1, respectively (Biswas et al. 2016). Besides, some important genes were related to the terpenoid biosynthesis including acetyl-CoA-acetyltransferase (*AACT*), 3-hydroxy-3-methyl glutaryl coenzyme A reductase (*HMGR*), and 1-deoxy-D-xylulose-5-phosphate synthase (*DXS*) targeted by the miR5072 (Xu et al. 2015), miR1134 (Fan et al. 2015), and miR156 (Singh et al. 2016). Moreover, some transcription factors, such as myeloblastosis (*MYB*) and SQUAMOSA promoter-binding protein-like (*SPL*) proteins play crucial roles in the regulation of the biosynthesis of flavonoids, anthocyanins and terpenoids. Gene encoding transcription factors mentioned above are targeted by the miRNAs, just as *MYB* and *SPL* targeted by miR858, miR159, and miR156, respectively (Yu et al. 2015; Sharma et al. 2016).

Although the miRNAs have been identified in many medicinal plants, no reports are available at present on the miRNAs of *T. sinensis*. Toon sprouts are rich in flavonoids and anthocyanins. However, the flavonoid content varies among the different *T. sinensis* varieties. Our prior works showed that the total flavonoid and anthocyanin concentrations in the BYC2 were remarkably higher than those in the

GYC2 (Zhao et al. 2017). Therefore, the two *T. sinensis* varieties provided an ideal model for a clear understanding of the miRNA-mediated regulation of the flavonoid biosynthesis at the post-transcriptional level. Besides, the unique flavor of the toon sprouts or shoots is closely related to the formation of its volatile terpenoids (Zhao et al. 2019). However, it is not clear that the miRNAs participate in the molecular events of the post-transcriptional regulation of the terpenoid biosynthesis in toon sprouts. The present study focuses on the identification of miRNAs and their targets together with our earlier transcriptome data in two toon sprout cultivars, i.e., the BYC2 vs GYC2. These results of this study revealed the expression profiles and regulation patterns of miRNAs involved in the flavonoids and terpenoids biosynthesis of toon sprouts. The miRNAs, which play potentially important roles in the formation of secondary metabolites, were identified and analyzed in toon sprouts, and their expression levels were experimentally validated by quantitative real-time PCR (qRT-PCR). To the best of our knowledge, this is the first report on sRNA high throughput sequencing in *T. sinensis*. Our results will be a valuable resource for the investigation of miRNA-mediated regulation of the flavonoids and terpenoids biosynthesis in toon sprouts.

Material and Methods

Plant Materials

Toon sprouts (the first and second leaves from the top sprouts) were randomly collected from two *T. sinensis* cultivars (BYC-2 vs. GYC-2) raised under natural environmental conditions in the *T. sinensis* industry demonstration zone at Taihe County, Anhui, China, in April 2019. Samples were collected according to our previous protocol (Zhao et al. 2017). The toon sprouts samples thus collected were immediately frozen in liquid nitrogen and stored at − 80 °C until future use for total RNA extraction, sRNA library construction and component analyses of the flavonoids and terpenoids.

Extraction and Determination of Flavonoid Constituents and Volatile Terpenoid

Fifteen toon buds of each cultivar were mixed as one replicate and three replicates were performed. The total flavonoid extractions and their quantification were performed per the protocol of Jiang et al. (2019). Briefly, 100 g of the toon sprout samples under refrigerator stored at − 80 °C were ground into powder with liquid nitrogen, and then immersed in 1000 mL acidified methanol (in a volume ratio of 1% HCl) for 24 h, under dark, at room temperature 20 °C. The extracts were then centrifuged at 12,000*g* for 20 min. The supernatant was drawn, and the residues were re-extracted twice with 300 mL of acidified methanol. Subsequently, the extracts were amalgamated together and concentrated to 30 mL under vacuum. Also, to remove the fat residue, the concentrated solution was extracted using petroleum ether (in a volume ratio of 1:2) three times; the hydrophilic phase was once dissolved in 30 mL of acidified methanol. The samples were filtered through a 0.22 μm polyethersulfone membrane filter before HPLC analysis. The flavonoid constituents were determined on a 1260 series HPLC instrument (Agilent, USA) equipped with Waters SunFire C18 Analytical Column (5 μm, 250 × 4.6 mm). All the flavonoid constituents were monitored under uniform protocol using a UV detector at 254 nm. A gradient of water and acetonitrile was used as the mobile phase at column temperature 30 °C with a flow rate of 0.8 mL/min. The time programs for gradient elution was as given: 0–15 min, 10–30% acetonitrile (A), 70-90% water (B); 15–30 min, 30-60% acetonitrile (A), 40-70% water (B); 30–35 min, 60-100% acetonitrile (A), 0-40% water (B). The chromatogram of the standard substance of the selected flavonoid constituents were purchased from Aladdin Company (Shanghai). To determined volatile terpenoids, GC–MS technology and corresponding experimental program used in our previous study were adopted and slightly modified (Zhao et al. 2019).

RNA Extraction, Quality Control, Small RNA Library Construction and Sequencing

The total RNAs of the toon sprouts were extracted from four samples (two biological repetition per cultivar) using RNAprep Pure Plant Kit (Tiangen Biotech, Beijing). To ensure the high quality of the RNA samples for sequencing, the quality of the total RNAs was assayed as follows: (1) RNA degradation and contamination was checked on 15% denaturing polyacrylamide gels. (2) RNA purity was monitored using the Thermo Scientific™ NanoDrop™ 2000 spectrophotometer (Thermo, Waltham, MA). (3) RNA concentration was assayed using a Qubit®RNA Assay Kit in Qubit®2.0 Fluorometer (Life Technologies, CA, USA). (4) RNA integrity was checked using the RNA Nano 6000 Assay Kit of the Bioanalyzer 2100 system (Agilent Technologies, CA, USA). After all the RNA samples were qualified, small RNA libraries were constructed using the TruSeq® Small RNA Sample Prep Kit. To accomplish this, 1 μg of total RNA per sample was used as the starting material to prepare the small RNA (sRNA) sequencing library. Briefly, 3′ adaptors were ligated to the specific 3′OH group of the small RNA followed by the 5′ adaptor ligation using the T4 RNA ligase. The ligated products were reversely transcribed by reverse transcriptase and special primers, enriched by PCR and the amplified products were electrophoresed on 15% urea polyacrylamide gel followed by sizes of the 140–200 bp fragment selected.

The small RNA library was quantified using NanoDrop and validated for quality by assaying the insert size using the Agilent 2100 bioanalyzer. Finally, Q-PCR was used to quantify accurately the effective concentration of the library (the effective concentration of the Library > 2 nM) to ensure its quality. Sequencing libraries were generated for Illumina sequencing (NEB, USA) following the manufacturer's recommendations and index codes were added to attribute sequences to each sample. Clustering of the index-coded samples was performed on a cBot Cluster Generation System using TruSeq PE Cluster Kit v4-cBot-HS (Illumina), according to the manufacturer's instructions. After cluster generation was complete, the library preparations were sequenced on an Illumina Hiseq 2500 platform and single-end 50 nt reads were generated (Beijing Novogene Technologies Co., Ltd, Beijing, China). All small RNA raw sequences from the GYC2_1, GYC2_2, BYC2_1, and BYC2_2 of the two varieties toon sprout libraries have been deposited in the Sequence Read Archive of NCBI with the corresponding accession numbers SRR12778803, SRR12778802, SRR12778801, and SRR12778800.

Prediction of Known and Novel miRNAs

After the sequencing run was completed, the raw data were first processed through the custom perl and python scripts. Clean data were obtained by removing the reads containing ploy-N, with 5' adapter contaminants, 3' adapter reads or the insert tag, less than 18 nt sequences and other low-quality reads from the raw data. The Rfam database was used to annotate and thus predict the non-coding RNAs such as the rRNA-, tRNA-, snRNA-, and snoRNA-derived sequences, etc. Next, the remaining sRNA sequences were mapped to the *T. sinensis* transcriptome sequence using the Bowtie software without mismatch, to analyze their expression and distribution on the reference (Langmead et al. 2009). The mapped sRNA tags were converged onto the miRBase v22.1 (http://www.mirbase.org/) for identification of the conserved miRNAs with zero mismatches, using the miRDeep2 software. After obtaining the known miRNAs and completing the family classification, the remaining sRNA sequences without annotation were used to predict the potential novel miRNA candidates. Initially, the sRNA reads were aligned with the *T. sinensis* transcriptome sequence using Bowtie. The characteristics of the hairpin structure of the miRNA precursor can be used to predict the novel miRNA. The available software miREvo and miRDeep2 were integrated to predict the novel miRNA by exploring the secondary structure (Friedlander et al. 2011; Wen et al. 2012). The reference standards for identifying the novel *T. sinensis* miRNA precursors were as follows (Meyers et al. 2008; Axtell and Meyers. 2018): (1) secondary stem-loop structure; (2) mature miRNA located in one arm of the stem, complementary sequence portion with the miRNA located on the opposite other arm, and termed miRNA*; (3) the miRNA/miRNA* duplex had no loop or break and possessed less than 6 base mismatches; (4) higher negative MFEI values of the miRNA precursors than the other RNAs; and (5) two nucleotides 3' overhang in the miRNA: miRNA* duplex. The Dicer cleavage site and minimum free energy of the sRNA tags were identified in the former steps. At the same time, custom scripts were employed to obtain the miRNA counts identified as well as the base bias on the first position, with certain length.

T.sinensis miRNA Expression Profiles, miRNA Target Identification and Function Annotation

The expression levels of both the known miRNAs and novel miRNAs from the buds of two toon cultivars were estimated by Transcripts Per Million (TPM) and normalized through the following criteria normalization formula (Zhou et al. 2010). Normalized expression = mapped miRNA counts / total clean read counts $\times 10^6$. Differential expression analysis between the BYC2 and GYC2 was performed using the DEGseq (2010) R package. The miRNAs having $p < 0.05$ and |log2-fold| change ≥ 1 in comparison, were set as the threshold for significantly differentially expressed miRNAs (DE-miRNAs) (Audic and Claverie. 1997; Baggerly et al. 2003). Blasting against the transcriptome data of the earlier reported two *T. sinensis* cultivars, a prediction of the potential target genes of the miRNA was done using the psRobot (http://omicslab.genetics.ac.cn/psRobot/) (Wu et al. 2012). Rigorous criteria were adhered to, as follows: mismatches between the miRNA/target were not to exceed four (G-U bases set as 0.5 mismatches); no more than two adjacent mismatches and 2.5 mismatches in positions 1–12 between 5' of the miRNA and target were permitted, and specifically, no adjacent mismatches were to be present in positions 2–12, as well as mismatches in positions 10–11; the minimum free energy (MFE) of the miRNA/target duplex should be not < 60% compared to the MFE of the miRNA bound to its perfect complement. Targets were also functionally annotated by BLASTX (*e* value $1 \times e^{-10}$) against the UniProtKB/Swiss-Prot and UniProtKB/TrEMBL databases for plants in our previous transcriptome data (Zhao et al. 2017). Gene ontology (GO) annotation for the targets of DE-miRNAs was done using the WEGO software (http://wego.genomics.org.cn/) (Ye et al. 2018). The targets of DE-miRNAs were mapped to the KEGG database (http://www.genome.jp/kegg/) to identify those genes involved in the flavonoid and terpenoid pathways (Kanehisa et al. 2017).

Expression Analysis of the miRNAs and Target Genes in Toon Sprouts by qRT-PCR

The miRNAs were extracted from the toon sprouts using the miRcute miRNA Isolation Kit (Tiangen Biotech, Beijing) according to the manufacturer's instructions. The total RNA of the toon sprouts for qRT-PCR was isolated adopting the protocol similar to the one in the previous experiment for total RNA quality control for sRNA sequencing. The miRNA poly (A) tailing and RT-PCR amplifications were performed using the miRcute Plus miRNA First-Strand cDNA Kit (Tiangen Biotech, Beijing). The RT-PCR amplifications for the target RNAs were performed using Quantscript RT Kit (Tiangen Biotech, Beijing) following the manufacturer's instructions. The qRT-PCR of the miRNA and target genes were performed in Step One Plus Real-Time PCR Systems (Thermo Fisher Scientific, Shanghai, China) using the miRcute Plus miRNA qPCR Kit (SYBR Green) (Tiangen Biotech, Beijing) and GoTaq-qPCR Master Mix Kit (Promega, Beijing, China), respectively. The primers for qRT-PCR were designed using Primer-BLAST (https://www.ncbi.nlm.nih.gov/tools/primer-blast/) and synthesized by Sunya Biotechnology Company (Hangzhou). The primer sequences for the miRNAs and their targets are listed in Supplementary file 8. The 20 µLvolume of the reaction mixture contained 2 µL of the dilute template cDNA, 2 µL of the primer pairs, 10 µL of 2 × miRcute Plus miRNA PreMix (containing 2 µL of 50 × ROX reference dye II), and 6 µL of deionized water. The setting program of the qRT-PCR reaction for the miRNA quantity was as follows: denaturation at 95 °C for 15 min, followed by 40 cycles of 94 °C for 20 s, annealing and extension at 60 °C for 34 s. For the target ungenes, the reaction system and PCR parameters were set according to our previous criterion and procedures (Zhao et al. 2017). After the reactions, primer specificity was evaluated by the melting curve analysis. The miRNAs and corresponding target genes in the qRT-PCR quantity were analyzed in three biological replicates and three technical replicates. The relative abundance of the miRNAs and target genes was determined using the $2^{-\Delta\Delta CT}$ method and normalized by U6 rRNA and β-actin as reference genes, respectively.

Statistical Analysis

The statistical analyses of the DEGs and DE-miRNA profiles were performed using *SPSS* 19.0 (Chicago, IL, CA). Student t-test was used to assess for the potential differences between the BYC2 and GYC2. $^{*}P < 0.05$ represented the statistically significant difference. The values were expressed as mean ± SD.

Results

Determination of Quality-Related Flavonoid and Terpenoid Contents in Toon Sprouts

The contents of the flavonoid in the toon sprouts of the BYC2 and GYC2 varieties were determined by the HPLC method (Table 1). The contents of the total flavonoid in the BYC2 and GYC2 were found to be 5722.13 ± 196.80 µg/g and 4936.72 ± 249.54 µg/g, respectively. The contents of six flavonoid monomers (except for rutin) namely, myricitrin, isoquercitrin, quercetin-3-O-α-L-arabinopyranoside, kaempferol-3-O-β-D-glucopyranose, quercitrin, and kaempferol-3-O-α-L-rhamopyranoside in the BYC2 were found to be 19.6, 38.3, 25.2, 32.8, 7.9, and 18.0% higher than those in the GYC2. However, the contents of the volatile terpenoid compounds between the two cultivars displayed a various change pattern (Table 2). The contents of the monoterpenoids such as α-pinene and d-limonene contents were significantly higher in the GYC2 than in the BYC2. Some important sesquiterpenoids such as the contents

Table 1 The contents of the flavonoid components (µg/g of fresh weight) in BYC2 and GYC2

Flavonoid components	Rt (min)	Molecular weight	Toon sprout cultivars (µg/g)	
			BYC2	GYC2
Myricitrin	8.145	464.38	314.11 ± 4.67	262.60 ± 6.31*
Rutin	9.384	610.52	992.37 ± 32.03*	1249.55 ± 41.33
Isoquercitrin	9.984	464.38	1765.06 ± 91.93	1276.37 ± 159.47*
Quercetin-3-*O*-α-L-arabinopyranoside	10.934	434.35	1664.78 ± 87.21	1329.76 ± 95.46*
Kaempferol-3-*O*-β-D-glucopyranose	11.920	448.38	411.12 ± 25.00	309.66 ± 9.74*
Quercitrin	14.379	448.38	274.14 ± 2.10	254.00 ± 2.51*
Kaempferol-3-*O*-α-L-rhamopyranoside	16.363	432.38	300.55 ± 4.41	254.76 ± 3.78*
Sum			5722.13 ± 196.80	4936.72 ± 249.54*

Values are expressed as the means of three replicates ± standard deviation

*Statistically significant differences for the flavonoid components in BYC2 and GYC2 ($^{*}P < 0.05$; Student's *t* test)

Table 2 The contents of volatile terpenoid compounds (ng/g of fresh weight) in BYC2 and GYC2

Peak	*R* t (min)	Volatile terpenoid compounds	Toon sprout cultivars (ng/g)	
			BYC2	GYC2
1	5.48	α-Pinene	24.13 ± 1.22*	129.54 ± 7.33
2	10.87	D-Limonene	198.36 ± 22.72*	224.31 ± 10.28
3	15.35	α-Cadinene	154.51 ± 9.51	143.56 ± 17.58
4	16.03	Ylangene	159.12 ± 14.86*	265.74 ± 21.58
5	16.23	α-Copaene	1116.28 ± 71.89*	1302.06 ± 17.67
6	16.47	α-Bourbonene	113.08 ± 7.98	89.57 ± 6.85*
7	16.61	β-Elemene	193.79 ± 8.35	135.46 ± 3.05*
8	17.12	β-Caryophyllene	3396.88 ± 235.22*	6215.39 ± 523.33
9	17.54	Caryophyllene	247.83 ± 30.66*	558.26 ± 89.48
10	17.67	trans-β-Farnesene	896.35 ± 24.09*	1355.90 ± 126.34
11	17.96	α-Guaiene	605.26 ± 37.75	141.92 ± 13.93*
12	18.14	α-Bisabolene	153.23 ± 12.44	133.13 ± 7.43*
13	18.50	α-Farnesene	366.48 ± 25.09*	1441.96 ± 123.35
14	18.60	α-Humulene	785.16 ± 47.53*	973.81 ± 85.13
15	18.73	Alloaromadendrene	200.97 ± 9.21	127.83 ± 9.27*
16	19.13	γ-Muurolene	650.17 ± 14.94	327.87 ± 12.77*
17	19.21	trans-β-Ionone	666.03 ± 62.08	366.27 ± 1.34*
18	19.30	α-Curcumene	404.15 ± 7.58	484.03 ± 106.11
19	19.78	δ-Humulene	428.40 ± 29.98*	813.07 ± 97.86
20	19.97	cis-α-Farnesene	667.20 ± 28.87*	1845.28 ± 128.64
21	20.09	β-Bisabolene	384.79 ± 16.78	377.86 ± 9.34
22	20.41	d–Cadinene	1680.22 ± 47.32	1547.95 ± 54.15*
23	20.51	Calamenene	1158.16 ± 15.31*	1469.36 ± 72.17
24	20.66	Dihydroactinidiolide	286.94 ± 10.69	203.15 ± 9.45*
25	20.93	α-calacorene	120.14 ± 14.07*	254.80 ± 19.59
26	21.07	Ledene oxide	113.14 ± 12.23*	340.17 ± 16.20
27	21.38	Isocalamendiol-dehydroxy	112.13 ± 26.26*	221.63 ± 15.38
28	22.35	Aromadendrene-dehydro	332.30 ± 46.41*	407.46 ± 30.57
29	22.62	α-Bulnesene	85.98 ± 8.54*	101.21 ± 3.12
30	23.38	Caryophyllene oxide	69.78 ± 10.75*	125.90 ± 2.38
31	24.45	Alloaromadendrene oxide-	163.13 ± 4.73*	598.94 ± 83.45*
32	31.12	Isolongifolene, 9,10-dehydro	2503.93 ± 44.81*	3644.33 ± 324.09
33	34.41	Isoaromadendrene epoxide	1343.32 ± 100.30	104.40 ± 16.09*
Sum			19,781.34 ± 556.61*	26,472.12 ± 1163.02

Values are expressed as the means of three replicates ± standard deviation

Statistically significant differences for terpenoid compounds in BYC2 and GYC2 ($P < 0.05$; Student's *t* test)

of β-caryophyllene, caryophyllene, trans-β-farnesene, α-farnesene, and isolongifolene, 9,10-dehydro in GYC2 were found to be 83.0, 152.3, 51.3, 293.5, and 45.5% higher than those in the BYC2, respectively. Moreover, β-caryophyllene showed the highest accumulation in the GYC2, with an absolute value of 6215.39 ± 523.33 ng/g achieved.

High Throughput Sequencing of Small RNA Libraries of T. sinensis

In this study, the four sRNA libraries were constructed and sequenced using two toon sprout cultivars (BYC2 vs. GYC2) with two biological replicates per cultivar. As shown in Table 3, the total raw data of 19,174,385, 23,020,318, 13,560,132, and 16,930,140 reads were generated in four libraries, namely, the GYC2_1, GYC2_2, BYC2_1, and BYC2_2, respectively. After adapter removal and low-quality data (sequence < 17

Table 3 Analysis of the small RNA sequencing from the toon sprouts of BYC2 and GYC2

	GYC2_1	GYC2_2	BYC2_1	BYC2_2
Total raw reads	19,174,385	23,020,318	13,560,132	16,930,140
Clean reads	18,596,858	22,252,682	13,056,247	15,791,016
Total small RNA reads	12,239,853	14,251,756	8,964,927	8,118,129
Mapped small RNA reads	11,341,399	12,582,255	7,539,982	6,815,160
Total unique reads	781,957	952,515	487,413	516,365
Mapped total pre-miRNA small reads	40,682	41,057	66,362	76,624
Mapped unique pre-miRNA small reads	868	1,277	874	818
Mapped hairpin	584	641	572	593
Mapped mature miRNA	250	295	261	225
rRNA, tRNA, snRNA, and snoRNA (mapped reads count)	4,207,049	4,385,655	2,078,935	1,734,949

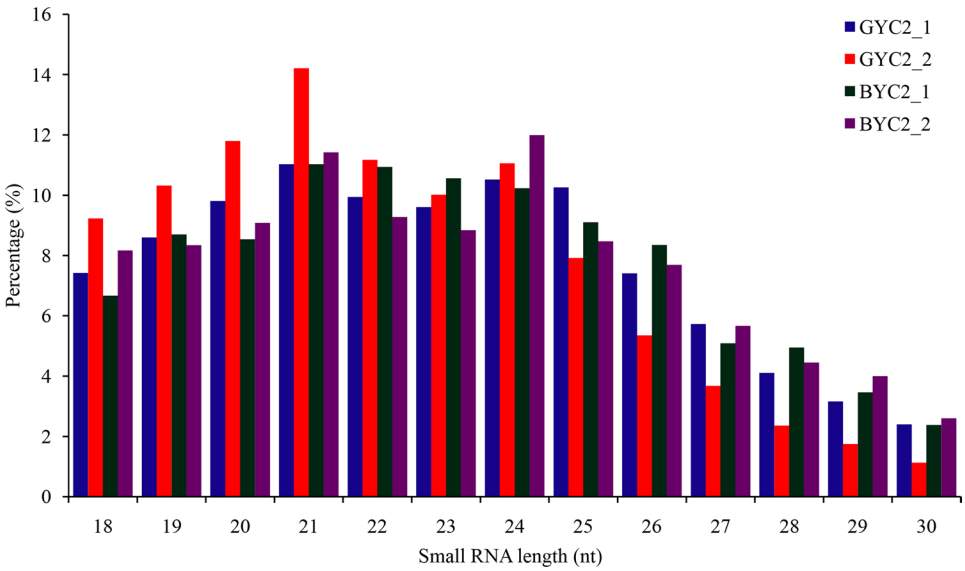

Fig. 1 Length distribution of clean reads of four small RNA libraries in BYC2 and GYC2

nt) filtering, 18,596,858, 22,252,682, 13,056,247, and 15,791,016 clean reads were obtained, with the total small RNA reads being in the proportion of 65.82% (12,239,853), 64.05% (14,251,756), 68.66% (8,964,927), and 51.41% (8,118,129) in each library. The read length distribution was centered mainly around 20–24 nt and contained over 60% of the total reads. As depicted in Fig. 1, the most abundant read length was 21 nt (11.03%-14.21%), followed by 24 nt (10.23%-11.99%) and 22 nt (9.28%-11.17%) (Fig. 1). Among them, 487–953 thousand unique reads corresponding to 7.54–12.58 million (about 83.95–92.66% of the total sRNA) reads were perfectly mapped to the *T. sinensis* transcriptome. The different types of the total sRNA sequences were further classified using the Bowtie software to blast the clean reads against the Rfam databases. The total counts of the annotated clean reads as tRNA, rRNA, snRNA, and snoRNA were 4,207,049, 4,385,655, 2,078,935, and 1,734,949 in GYC2_1, GYC2_2, BYC2_1, and BYC2_2, respectively. The remaining clean reads were aligned and edited in the Sequence Alignment Map (SAM) format and input into the miRDeep2 pipeline for the discovery of miRNA. In comparison, 818–1,277 unique reads corresponding to 40,682–76,624 reads were matched to the miRBase database. In total, 250–295 reads were found to match the known mature miRNAs collected from all plant species available in the miRBase database or be recognized as novel miRNAs in the *T. sinensis* transcriptome according to the miRDeep2 software.

Identification of Known miRNAs in T. sinensis Sprouts

To further identify the miRNA homologs in the *T. sinensis* sprouts, the remaining clean reads in the four libraries were aligned to the known miRNA in the miRBase (Release 22.1). 60,900, 70,254, 35,736, and 45,105 reads from

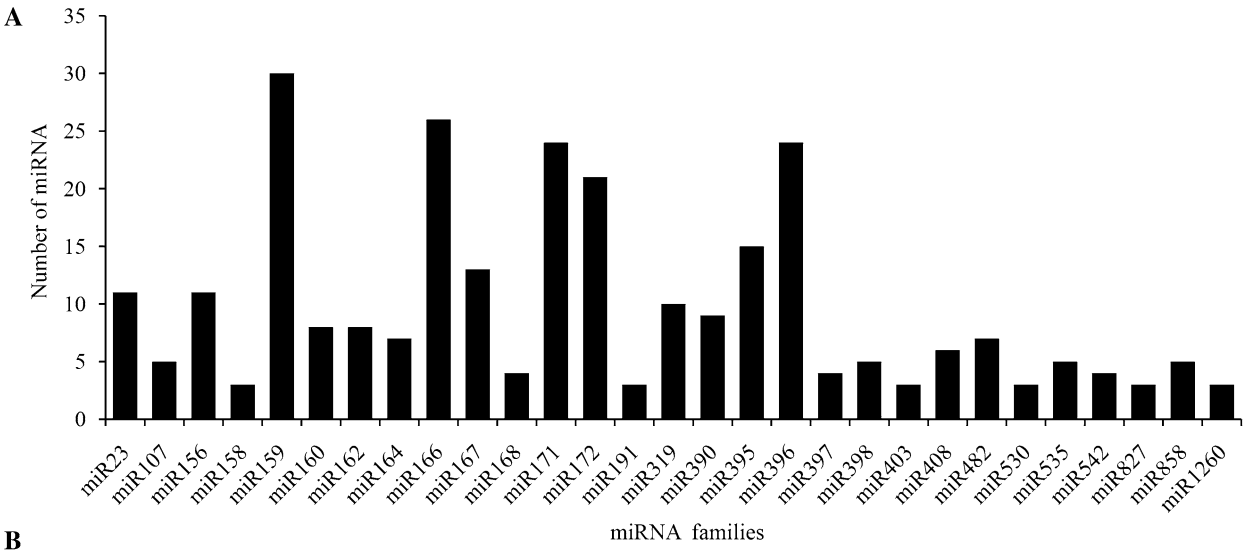

B

Known miRNA families of one member	miR169	miR186	miR376	miR393	miR414	miR529
	miR1511	miR2118	miR2673	miR2916	miR3533	miR3601
	miR3629	miR3711	miR3954	miR4784	miR4995	miR5083
	miR5368	miR5583	miR5658	miR6173	miR6478	miR8117
	miR8155	miR8577	miR9341	miR10760	miR11602	
Known miRNA families of two members	miR103	miR157	miR165	miR330	miR394	miR574
	miR1843	miR3630	miR4414	miR5139	miR7398	

Fig. 2 Known miRNA families and their member numbers in the toon sprouts. **A** The x-axis represents the members in the different miRNA families. The y-axis shows the conserved miRNA family identified in the BYC2 and GYC2. **B** 29 and 11 miRNA families included only one or two members

BYC2_1, BYC2_2, GYC2_1 and GYC2_2 libraries perfectly matched 243, 208, 230, and 275 known mature miRNAs, respectively. The total number of known miRNAs in the GYC2 was slightly higher than those present in the BYC2. In total, 331 known miRNAs belonging to 56 families were identified in the four libraries, with an average of about six miRNA members per family (Fig. 2A). Among these known miRNA families, only one member was identified in 29 miRNA families, while two members were identified in 11 miRNA families (Fig. 2B). However, some miRNA families possessed several members. For example, miR159 was the largest family containing 30 members, followed by miR166, miR171and miR396 with 26, 24, and 24 members, respectively (Fig. 2A). These known miRNAs were aligned to all the plant species available in the miRBase database, among which *Arabidopsis thaliana*, *Oryza sativa*, and *Glycine max* were the most frequent ones. The transcript numbers of these miRNAs in the toon sprouts varied greatly among the miRNA families. Some only had several sequence reads, whereas others possessed hundreds of thousands of reads. For example, most members of the miR166 family possessed more than 20,000 reads, and some of the miR166 family and most members of the miR159 family had more than 5,000 reads, and most of the miR159, miR319 and miR482 families possessed more than 2,000 read, while the majority of the other miRNAs had only a few hundred, or even fewer reads has been furnished in Supplementary file 1.

Identification of Novel miRNAs in Toon Sprouts

The remaining sRNAs that were unannotated to the miRBase were searched against the *T. sinensis* transcriptome, using the miRDeep2 software to identify the novel miRNAs that may be specific to the toon sprouts. Based on the recognition criteria of the potential novel miRNA precursor, a total of 23 novel miRNAs were identified in the four sRNA libraries (Table 4). The novel miRNA sequences varied in the range of 18–24 nt, with an average length of 21 nt. The pre-miRNAs lengths varied in the range of 53–293 nt, with the average being 130 nt. The average

Table 4 List of putative novel miRNAs in the toon sprout

Name	Sequence	Length (nt)	Arm	Position in gene ID	Precursor length (nt)	Energy (kcal/mol)
novel_1	UUGCGAUGUAGUACAAGAUG	20	3p	Unigene19347_All:297..453:-	156	− 54.9
novel_12	AUUUGUUUUGUGACAGUCAGAGUG	24	5p	Unigene19347_All::22..223:-	201	− 48.3
novel_13	UUUUUCCCACUCCUCCCAUUCC	22	3p	Unigene27585_All:823..902:-	79	− 27.5
novel_18	UUCCACAGCUUUCUUGAACUU	21	5p	Unigene21991_All:144..263:+	119	− 43.1
novel_19	UGCAGGGGAGAUGACACCGUC	21	5p	Unigene896_All:488..567:-	79	− 30.8
novel_2	UUCCACGGCUUUCUUGAACGUAA	23	5p	Unigene5618_All:343..432:-	89	− 37.2
novel_20	UGAAUCCUGAUGAUGCUGCAU	21	3p	Unigene5618_All::128..200:-	72	− 24.4
novel_22	AGGAGAAAUGGGGAUGGGGAUGGG	24	5p	Unigene5618_All::1..54:-	53	− 35.2
novel_23	UGCUCAUAUCUCUUUCUGUCAG	22	3p	Unigene5618_All::18..98:-	80	− 40.6
novel_24	UUGACAGAAGACAGAGAGCAC	21	5p	Unigene5618_All::22..106:-	84	− 39.4
novel_25	CUUGAACGCGGUGGCUCA	18	5p	Unigene8425_All:444..737:+	293	− 111.3
novel_26	UCUUUCCCACUCCUCCAAUUCC	22	3p	Unigene1154_All:505..581:-	76	− 34.7
novel_27	UUCUUCUGUUUUCUUGGUAAC	21	3p	CL9194.Contig3_All:3500..3596:-	96	− 22.86
novel_28	GCUCUGAAUGUCAAAGUG	18	5p	Unigene4740_All:554..738:+	184	− 64.74
novel_3	CAUGCAUAUCUCAGGAGCUUC	21	3p	CL3421.Contig3_All:624..711:-	87	− 35.4
novel_31	UCCUGUGACUUCCUGUAGUUCC	22	3p	Unigene24408_All:267..381:-	114	− 41.9
novel_32	UUUCUGAUUUUAGUAGUACUGA	22	3p	CL8451.Contig2_All:1162..1362:+	200	− 64.7
novel_33	UUGCCAACACCUCCGAUGCCGA	22	3p	Unigene19197_All:207..310:+	103	− 30.7
novel_34	UGGUUGGUCUGUUGGUGCC	19	3p	CL2802.Contig3_All:1227..1499:+	272	− 85.2
novel_5	UUUCCAAUUCCUCCCAUCCCUA	22	3p	CL2802.Contig3_All:55..137:+	82	− 28.96
novel_7	UUUCCAAUCCCUCCCAUCCCUA	22	3p	CL2802.Contig3_All:136..215:+	79	− 30.4
novel_8	UUUGGAUUGAAGGGAGCUCU	20	5p	CL3421.Contig2_All:688..975:+	287	− 65.04
novel_9	AGCUCUGUUGGUUUCUCUUUG	21	3p	CL10828.Contig1_All:225..351:-	126	− 42.65

Table 5 Nucleotide composition and bias for the first position of the novel miRNAs with different length from the 5' end of the sequences

First base	miRNA length (nt)							
	18	19	20	21	22	23	24	Total
A				1			2	3
U		1	2	5	8	1		17
C	1			1				2
G	1							1
Total	2	1	2	7	8	1	2	23

minimum folding free energy value of the hairpin structures was −45.22 kcal/mol in the toon sprouts, which is higher than that reported in *Arabidopsis* (−59.50 kcal/mol). The secondary structures of the 23 novel miRNA precursors have been furnished in Supplementary file 2. As shown in Table 5, the first nucleotide base analysis indicated that a large majority of the novel miRNAs started the first nucleotide with 5' uracil (U) not guanine (G) and U (73.91%) were the most dominant nucleotides in the first position, which is consistent with the typical miRNA nucleotide bias distribution patterns.

Differential Expression of the miRNAs Between the Two Toon Sprout Varieties

Pairwise analysis of the DE-miRNAs between the BYC2 and GYC2 was performed using the heat map method (Fig. 3). There were totally 52 (25 up-regulated, and 27 down-regulated) significantly DE-miRNAs between the BYC2 vs GYC2 ($\log_2$ ratio ≥ 1, adjusted P value ≤ 0.05). Among these, the miR166, miR168, miR408, and miR482 and novel miRNAs 5, 7, 13, 23, and 33 were up-regulated, while the miR156, miR171, miR172, miR394, miR396, miR403, miR858 families together with the novel miRNAs 3 and 27 were down-regulated between the BYC2 and

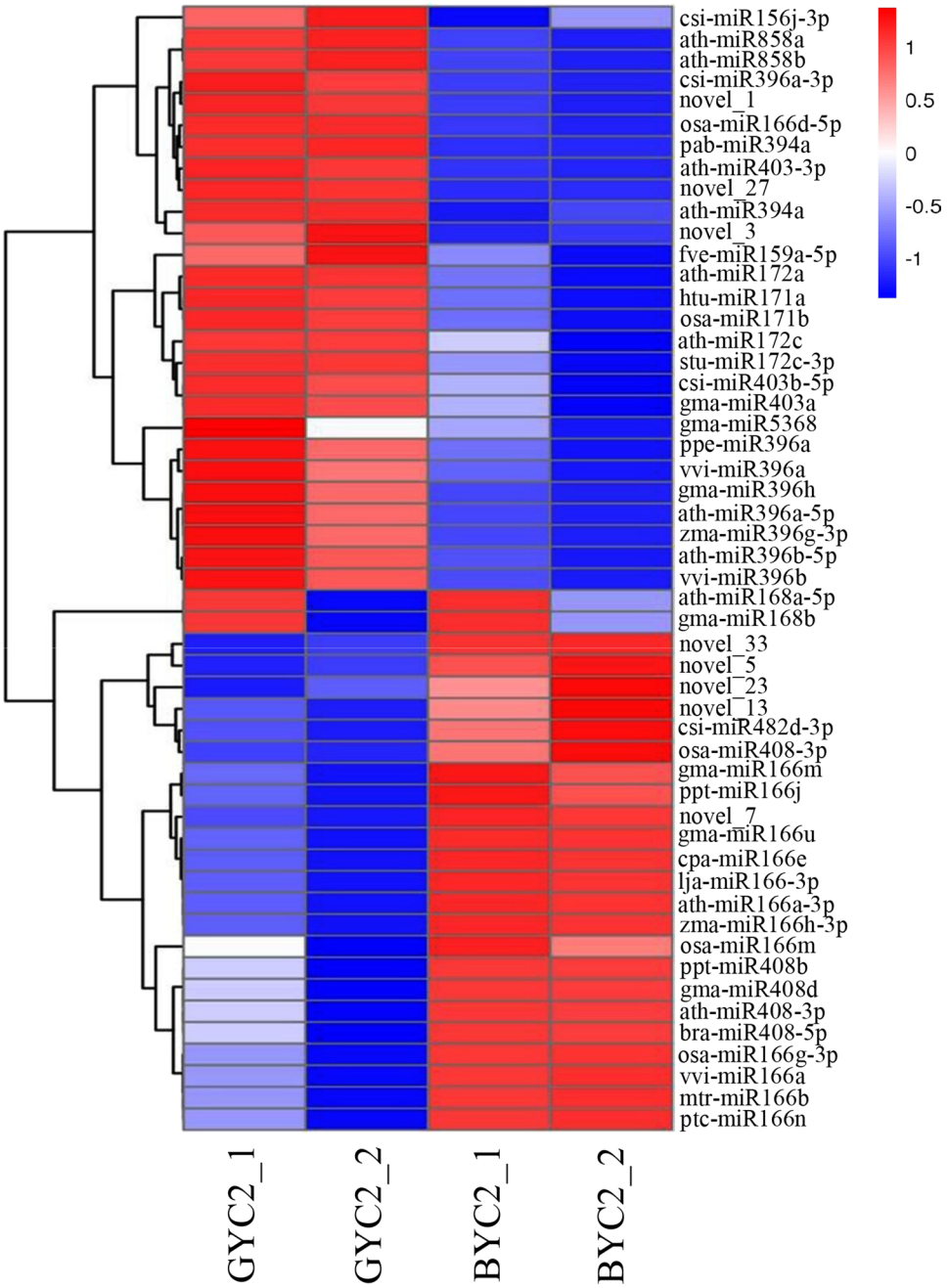

Fig. 3 Clustering analysis of the DE-miRNAs was shown using heatmap. Heatmap represents the miRNAs significantly altered by the Baggerley's test ($P < 0.05$) in four libraries. The blue color indicates low expression of the miRNAs, while red indicates the high expression of the miRNAs

GYC2 (Supplementary file 3). Interestingly, the levels of DE-miRNAs were found to be remarkably different among the different miRNA families. For example, the miR166, miR172, miR156 and miR858 exhibited greater differential expression than did the miR396 and miR168. Moreover, different members of the same miRNA family displayed different expression levels. For example, the miR166a and miR166d exhibited significantly reverse expression patterns. Compared with the GYC2, the miR166a was significantly up-regulated in the BYC2, whereas the miR166d was significantly down-regulated (Supplementary file 3). It is noteworthy that some DE-miRNAs were predicted to play crucial roles in the regulation of the secondary metabolism in the toon sprouts.

Target Prediction and Functional Annotation

A total of 2233 target genes (or 18,224 transcripts of 2233 target genes) of miRNAs were predicted in the toon sprouts using the psRNA Target software (Supplementary file 4). Moreover, a majority of the miRNAs possessed multiple target unigenes, and the target unigenes number of miRNAs varies greatly from 1 to 1986. For instance, tsi-miR156z (belonging to the miR156 family) topped the list with 1986

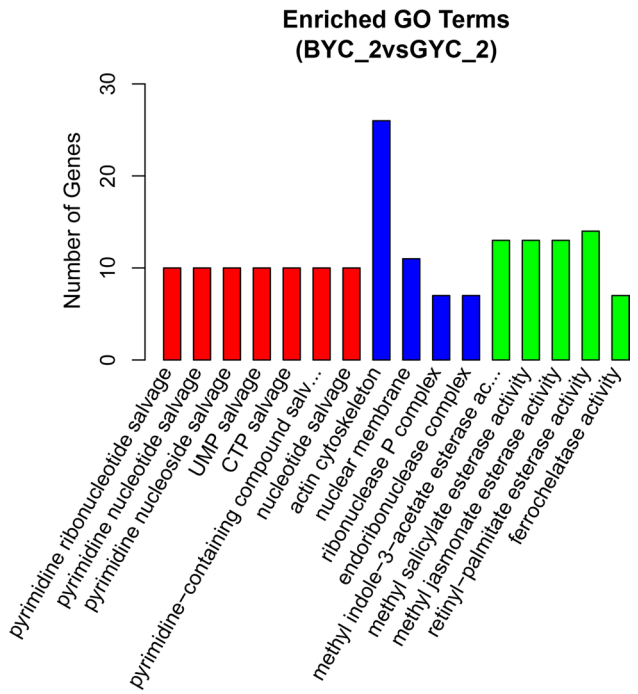

Fig. 4 Gene ontology (GO) enrichment was classified for the potential target unigenes of the DE-miRNAs. Red, blue, and green represent the three GOs, namely, biological progress, cellular component, and molecular function, respectively

target transcripts, followed by tsi-miR5658, tsi-miR414 and tsi-miR172c-3p which had 1915, 1781, and 1627 target transcripts, respectively. Among all the novel miRNAs, the novel_28 possessed the highest number of target transcripts (1377) while the lowest number of targets was found in novel_12 (36); these data have been furnished in Supplementary file 5.

To better understand the function of the miRNAs in the toon sprouts, the target unigenes of DE-miRNAs were annotated through the analysis of GO enrichment, (Supplementary file 6) and the KEGG pathway (Supplementary file 7: Table S5). The GO enrichment analysis showed that the target unigenes of DE-miRNAs appeared to be significantly enriched in the methyl indole-3-acetate esterase activity (GO: 0080030), methyl salicylate esterase activity (GO: 0080031), and methyl jasmonate esterase activity (GO: 0080032) in molecular function. Under biological process, pyrimidine ribonucleotide salvage (GO: 0010138), pyrimidine nucleotide salvage (GO: 0032262), UMP salvage (GO: 0044206), and CTP salvage (GO: 0044211) were significantly enriched. For the cellular component category, the actin cytoskeleton (GO: 0015629) and nuclear membrane (GO: 0031965) were determined to be highly represented groups (Fig. 4).

The KEGG pathway analysis demonstrated highly significant enrichment in the RNA transport, spliceosome, mRNA surveillance pathway, endocytosis, and RNA degradation (Fig. 5). Some metabolic pathways, including the other types of O-glycan biosynthesis, galactose metabolism, and purine metabolism, vitamin B6 and ascorbate metabolism, as well as essential amino acid and fatty acid biosynthesis were ranked among the top 20 enrichment pathways (Supplementary file 7). To identify a difference in the flavonoid contents between the BYC2 and GYC2, we focused on those miRNAs that may negatively regulate the unigenes associated with the flavonoid biosynthesis. In our study, there are key enzyme unigenes as potential targets regulated by *T. sinensis* miRNAs, such as cinnamic acid 4-hydroxylase (*C4H*), shikimate O-hydroxycinnamoyltransferase (*HCT*), dihydroflavonol-4-reductase (*DFR*), leucoanthocyanidin dioxygenase (*LDOX*), leucoanthocyanidin reductase (*LAR*), and anthocyanidin 3-O-glucosyltransferase (*UGT*) which were predicted to be targeted by the tsi-miR403-3p, tsi-miR168b, tsi-miR166a, tsi-miR395a, tsi-miR319i, tsi-miR172c, and tsi-miR396b, respectively. The novel_27 was predicted to be a mutual regulator of the targets in 4-coumarate CoA ligase (*4CL*), and chalcone synthase (*CHS*) (Table 6).

By mapping these target unigenes of DE-miRNAs to the KEGG pathway, some targets encoding putative enzymes in the terpenoid biosynthesis were identified in *T. sinensis*. For example, the upstream target enzymes were located in the biosynthesis of the terpenoid backbone, including 3-hydroxy-3-methylglutaryl-CoA reductase (*HMGR*), mevalonate kinase (*MK*), phosphomevalonate kinase (*PMK*), and farnesyl diphosphate synthase (*FPPS*) in the mevalonate (*MVA*) pathways in the cytoplasm and 1-deoxy-D-xylulose-5-phosphate synthase (*DXS*), and 4-hydroxy-3-methylbut-2-enyl-diphosphate synthase (*HDS*) in 2-C-methyl-D-erythritol-4-phosphate (MEP) in the plasmid. These unigenes were predicted to be targets by tsi-miR408-3p, tsi-miR171a, novel_28, tsi-miR390b-5p, tsi-miR-1260, and novel_27. The downstream targets belonged to the terpene synthases (*TPS*) in the terpenoid biosynthesis. For example, (R)-limonene synthase (*LS*) and linalool synthase (*LIS*) were targeted by tsi-miR395d and tsi-miR172c-3p in monoterpenoid biosynthesis. Terpene synthase 11 (*TPS11*), (E)-β-farnesene synthase (*FAS*), and (-)-germacrene D synthase (*GDS*) in the biosynthesis of sesquiterpenoid were targeted by the tsi-miR8155, tsi-miR482d-5p and tsi-miR395b-3p. Besides, a large number of transcription factors that could be involved in regulation of secondary metabolite biosynthesis, growth and development in the toon sprouts were predicted as the candidate targets of some conserved miRNA families. For example, the squamosa promoter-binding-like protein (*SPL*) transcripts (Yu et al. 2015), anthocyanin regulatory C1 protein (*MYB*) transcripts (Xia et al. 2012), WD40-repeat protein (*WD40*) transcripts, homeodomain leucine zipper family (*ZIP*) transcripts (Sharma et al. 2016), ethylene-responsive

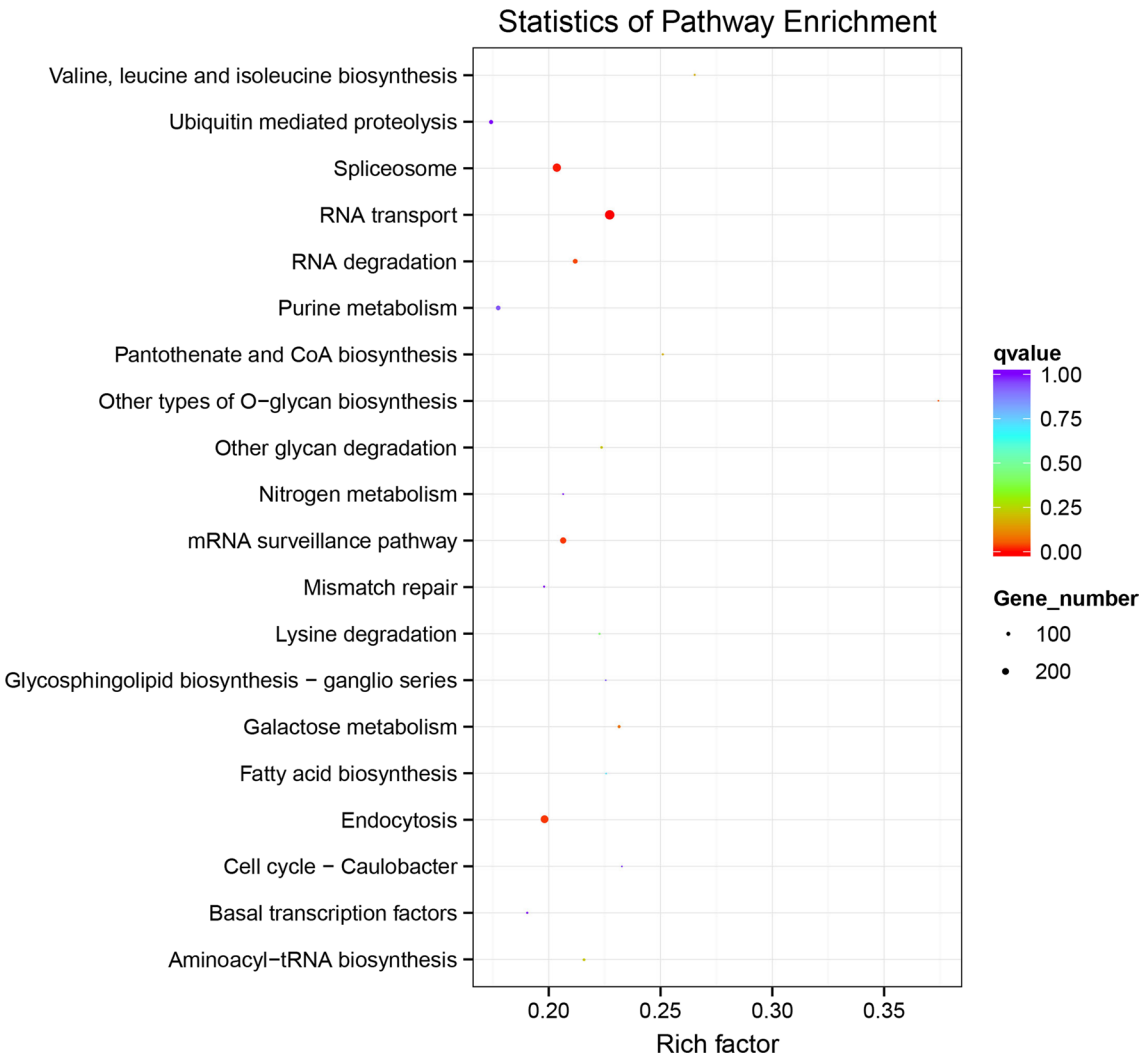

Fig. 5 Top 20 KEGG pathways enrichment was analyzed for the potential target unigenes of the DE-miRNAs. A large enrichment factor denotes a high degree of enrichment. The lower q-value represents the more significant enrichment of the DEGs

transcription factor (*ERF*) transcripts, WRKY transcription factor (*WRKY*) transcripts (Sun et al. 2017), and auxin response factor (*ARF*) transcripts were potentially targeted by the miR156, miR858, miR159, miR396, miR166, miR167, miR172, and miR160 families, respectively (He et al. 2019).

qRT-PCR Experimental Validation and Analysis of miRNAs and their Targets

The qRT-PCR was performed to validate the sRNA sequencing results and analyze the relationship between these miRNAs and their potential targets involved in the metabolic pathways of the flavonoid and terpenoid. Overall, the relative expression levels of the 40 miRNAs and 51 unigenes were quantified by the qRT-PCR. The qRT-PCR results of the miRNAs matched the expression profiles obtained by the sRNA sequencing, indicating that the sRNA sequencing data was credible and reliable. On the whole, the expression levels of the corresponding targets exhibited a trend opposite to those of the miRNAs (Figs. 6, 7, 8). In the flavonoid pathway, the tsi-miR4995, tsi-miR403-3p, novel_27, tsi-miR171c-5p, novel_34, tsi-miR172c, tsi-miR319i, tsi-miR408d, and tsi-miR396b showed significantly negative relationships with their responding target unigenes, *PAL*, *C4H*, *Trans-CMO*, *4CL*, *HCT-2*, *CHS*, *DFR*, *LDOX*, *LAR-1*, *LAR-2*, and *UGT* (Fig. 6). To explore the function of the miRNAs on the terpenoid biosynthesis in the toon sprouts, the expression profiles of the miRNA-target unigene pairs were selected for qRT-PCR analysis with P value < 0.05 as the significant difference. Among these, the expression level of 8 miRNAs was found to have a remarkably negative

Table 6 Potential targets involved in the flavonoid and terpenoid metabolism and their regulation for the miRNAs in the toon sprout

Metabolic pathways	miRNA ID	miRNA name	Target ID	Score	Annotation for targets	Gene name
Flavonoids-related miRNAs	gma-miR4995	tsi-miR4995	CL298.Contig3_All	6	Phenylalanine ammonia lyase	*PAL*
	ath-miR403-3p	tsi-miR403-3p	CL11631.Contig1_All	5.5	Cinnamic acid 4-hydroxylase	*C4H*
	novel_27	novel_27	CL8791.Contig1_All	6	4-coumarate: coenzyme ligase	*4CL*
	ata-miR395b-3p	tsi-miR395b-3p	CL5643.Contig1_All	5	Coumarate-3-hydroxylase	*C3H*
	gma-miR168b	tsi-miR168b	CL11692.Contig2_All	5	Shikimate *O*-hydroxycinnamoyltransferase	*HCT-1*
	ath-miR171c-5p	tsi-miR171c-5p	CL3044.Contig6_All	5.5	Shikimate *O* hydroxycinnamoyltransferase	*HCT-2*
	pta-miR159a	tsi-miR159a	CL8681.Contig4_All	6	Caffeoyl-CoA O-methyltransferase	*CCoAOMT*
	ath-miR403-3p	tsi-miR403-3p	CL11631.Contig1_All	5.5	Trans-cinnamate 4-monooxygenase	*Trans-CMO*
	novel_27	novel_27	CL6701.Contig1_All	6	Chalcone synthase	*CHS*
	novel_27	novel_27	CL2051.Contig1_All	6	Flavanone 3-dioxygenase	*F3H*
	vvi-miR166a	tsi-miR166a	CL9131.Contig1_All	5	Flavonol synthase	*FLS*
	novel_34	novel_34	CL4232.Contig2_All	5	Dihydroflavonol-4-reductase	*DFR*
	ath-miR172c	tsi-miR172c	CL6954.Contig1_All	6	Leucoanthocyanidin dioxygenase	*LDOX*
	ptc-miR319i	tsi-miR319i	CL11381.Contig1_All	4.5	Leucoanthocyanidin reductase	*LAR-1*
	gma-miR408d	tsi-miR408d	CL11381.Contig2_All	6	Leucoanthocyanidin reductase	*LAR-2*
	vvi-miR396b	tsi-miR396b	CL4956.Contig2_All	5	UDP-glycosyltransferase	*UGT*

Table 6 (continued)

Metabolic pathways	miRNA ID	miRNA name	Target ID	Score	Annotation for targets	Gene name
Terpenoids-related miRNAs	aqc-miR530	tsi-miR530	CL2271.Contig1_All	6	Acetyl-CoA acetyltransferase	*AACT*
	osa-miR408-3p	tsi-miR408-3p	CL1660.Contig2_All	6	3-hydroxy-3-methyl glutaryl coenzyme A reductase	*HMGR*
	htu-miR171a	tsi-miR171a	CL2366.Contig1_All	6	Mevalonate kinase	*MK*
	novel_28	novel_28	CL11364.Contig3_All	6	Phosphomevalonate kinase	*PMK-1*
	novel_22	novel_22	CL10814.Contig2_All	3.5	Phosphomevalonate kinase	*PMK-2*
	oar-miR-23b	tsi-miR-23b	CL9623.Contig2_All	6	Diphosphomevelonate decarboxylase	*PMDC*
	cgr-miR-1260	tsi-miR-1260	CL6132.Contig3_All	4	1-deoxy-D-xylulose-5-phosphate synthase	*DXS-1*
	ath-miR171c-5p	tsi-miR171c-5p	Unigene8467_All	6	1-deoxy-D-xylulose-5-phosphate synthase	*DXS-2*
	ath-miR414	tsi-miR414	CL3824.Contig1_All	3.5	2-C-methyl-D-erythritol 4-phosphate cytidylyltransferase	*MCT*
	mtr-miR2673a	tsi-miR2673a	CL716.Contig1_All	5.5	4-diphosphocytidyl-2-C-methyl-D-erythritol kinase	*CMK*
	novel_27	novel_27	CL10621.Contig1_All	6	4-hydroxy-3-methylbut-2-en-1-yl diphosphate synthase	*HDS*
	novel_28	novel_28	CL2055.Contig7_All	6	4-hydroxy-3-methylbut-2-enyl diphosphate reductase	*HDR*
	gma-miR395d	tsi-miR395d	CL10447.Contig2_All	6	Limonene synthase	*LS*
	gma-miR390b-5p	tsi-miR390b-5p	CL912.Contig1_All	5	Farnesyl diphosphate synthase	*FPPS*
	ipu-miR-107b	tsi-miR-107b	CL11437.Contig1_All	6	Geranyl diphosphate synthase	*GPPS*
	cas-miR156g	tsi-miR156g	CL10304.Contig4_All	5.5	Geranylgeranyl pyrophosphate synthase	*GGPPS-1*
	ama-miR396-3p	tsi-miR396-3p	CL10304.Contig3All	5	Geranylgeranyl pyrophosphate synthase	*GGPPS-2*
	cpa-miR8155	tsi-miR8155	CL5156.Contig1_All	5	Terpene synthase 11	*TPS11*
	csi-miR396e-5p	tsi-miR396e-5p	CL2694.Contig3_All	5.5	Linalool synthase	*LIS*
	csi-miR482d-5p	tsi-miR482d-5p	CL1924.Contig2_All	5	(E)-β-farnesene synthase	*FAS*
	ata-miR395b-3p	tsi-miR395b-3p	CL7579.Contig1_All	4	(-)-Germacrene D synthase	*GDS*
	novel_32	novel_32	CL7174.Contig3_All	4	Squalene synthase	*SQS*
	gra-miR166d	tsi-miR166d	CL6497.Contig6_All	5.5	Ent-kaur-16-ene synthase	*KS*
	vvi-miR396b	tsi-miR396b	Unigene4370_All	5.5	Squalene epoxidase	*SE*

Table 6 (continued)

Metabolic pathways	miRNA ID	miRNA name	Target ID	Score	Annotation for targets	Gene name
Transcription factor-related miRNAs	ath-miR156a-5p	tsi-miR156a-5p	CL1040.Contig5_All	1	Squamosa promoter-binding-like protein	*SPL1*
	ath-miR156a-5p	tsi-miR156a-5p	CL1666.Contig2_All	1	Squamosa promoter-binding-like protein	*SPL2*
	ath-miR858a	tsi-miR858a	CL598.Contig1_All	3	Anthocyanin regulatory C1 protein	*MYBC1-1*
	aqc-miR159	tsi-miR159	CL6837.Contig2_All	5.5	Transcription factor MYB1R1	*MYB1R1*
	ath-miR858a	tsi-miR858a	CL8713.Contig1_All	3	Anthocyanin regulatory C1 protein	*MYBC1-2*
	gma-miR159b-3p	tsi-miR159b-3p	CL3567.Contig2_All	0	Transcription factor GAMYB	*MYB*
	zma-miR396g-3p	tsi-miR396g-3p	CL190.Contig3_All	5.5	WD40-repeat protein	*WD40-1*
	ppt-miR167	tsi-miR167	CL5508.Contig3_All	4	WD40-repeat protein	*WD40-2*
	vvi-miR166a	tsi-miR166a	CL1000.Contig1_All	0.5	Homeobox-leucine zipper protein ATHB-15-like	*HD-ZIP*
	stu-miR172c-3p	tsi-miR172c-3p	CL4727.Contig1_All	6	Ethylene-responsive transcription factor	*ERF*
	stu-miR172c-3p	tsi-miR172c-3p	CL9023.Contig1_All	6	WRKY transcription factor	*WRKY*
	gma-miR160b	tsi-miR160b	CL2844.Contig1_All	0	Auxin response factor	*ARF*

correlation with their target unigenes including the tsi-miR-1260, novel_28, tsi-miR390b-5p, tsi-miR-107b, tsi-miR156g, tsi-miR8155, tsi-miR482d-5p, and tsi-miR395-3p, targeted for *DXS-1*, *HDR*, *FPPS*, *GPPS*, *GGPPS-1*, *TPS11*, *FAS*, and *GDS* (Fig. 7). Moreover, the other differentially expressed miRNA-target unigene pairs between the BYC2 and GYC2 were investigated in our study, and have been annotated as vital transcription factors in the regulation of secondary metabolism in plants, including SPL, MYB, WD40, WRKY, ERF, and ARF. A negative correlation was observed between the expression profiles of six miRNAs (tsi-miR156a-5p, tsi-miR858a, tsi-miR159, tsi-miR167, and tsi-miR172c-3p, and tsi-miR160b) and their targets *SPL1*, *SPL2*, *MYBC1-1*, *MYBC1-2*, *MYB1R1*, *MYB*, *WD40-2*, *ERF*, *WRKY*, and *ARF* (Fig. 8). The results stated above were consistent with our high-throughput sequencing data, which once again demonstrated that the credibility of our sRNA sequencing data.

Discussion

T. sinensis is one of the most highly valuable plants classified under Medicine Food Homology (MFH) in China. The natural properties among different varieties reveal significant diversity during evolution (Chen et al. 2018). In Taihe County of the Anhui Province of China, two fine *T. sinensis* strains were obtained, and extensively planted after a long cultivation and domestication history. One variety was called purple toon or "Black Youchun" (BYC2) for its rich flavonoid or anthocyanin, the other named green toon or "Green Youchun" (GYC2) for its strong aromas, is known as mahogany and used for architecture or furniture. Our study confirmed that the presence of significant differences in the total flavonoid contents between BYC2 and GYC2, with the flavonoid components ranging from 254.00 to 1765.06 μg/g of fresh toon sprouts. Rutin, isoquercitrin, and quercetin-3-*O*-α-L-arabinopyranoside are the three main representative components, known for their high abundance. The total flavonoid content in the BYC2 was higher than that in GYC2, which is consistent with their phenotypic property. However, compared with the flavonoids, the content of the volatile terpenoid in the GYC2 was higher than in the BYC2. The difference in the abundance of volatile terpenoid compounds between the BYC2 and GYC2 may account for their respective characteristics aromas.

To explore the biosynthesis pathways of flavonoid and terpenoid, transcriptome sequencing was performed earlier to explain the difference in the anthocyanin contents between the BYC2 and GYC2. The results showed that the expression levels of some principal genes related to the flavonoid biosynthesis were up-regulated more significantly in BYC2 than GYC2 (Zhao et al. 2017). The difference in the gene expression profiles could conspicuously contribute to the difference in the secondary metabolites in the toon sprouts. The miRNAs were considered to be

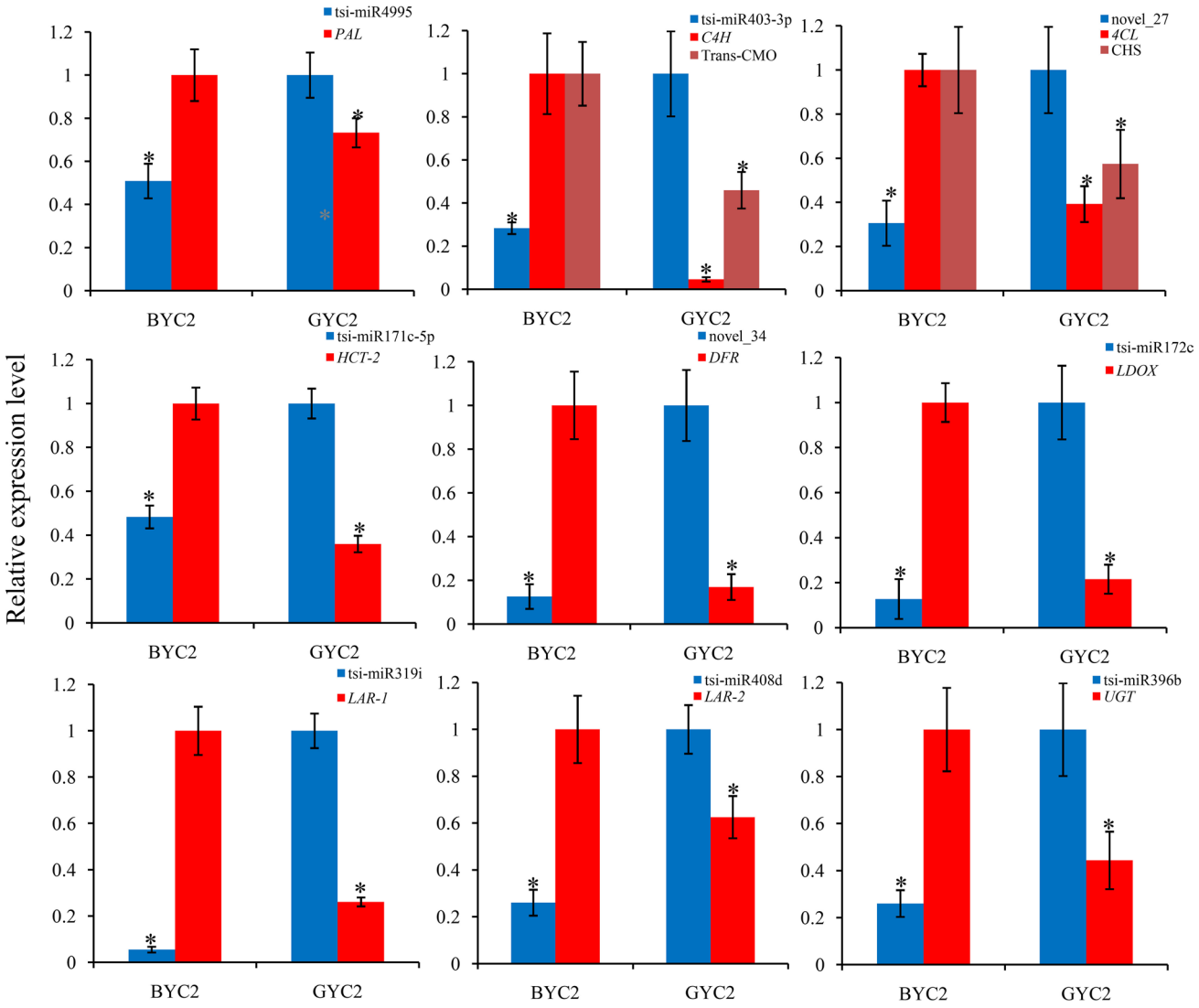

Fig. 6 The qRT-PCR validation of miRNAs and their target unigenes related to the flavonoid biosynthesis in BYC2 and GYC2. All the values represent an average ± SD ($n = 6$). The error bars with asterisks are the statistically significant differences (*$P < 0.05$; Student's t test)

in control of the vital physiological processes in plants, including the regulation of the secondary metabolic pathways, mainly at the post-transcriptional level. To the best of our knowledge to date, this is the first report on attempting to investigate and explore the miRNAs and their potential targets in *T. sinensis*. In view of the lack of genomic information for *T. sinensis*, high throughput RNA sequencing could be performed to reveal the miRNA-target pairs which control the metabolic flows of the flavonoid and terpenoid. To study the miRNA-mediated regulation of the gene expression at the post-transcriptional level in the toon sprouts, sRNA sequencing combined with the previous transcriptome data was done to identify the miRNA candidates and their potential targets. In this study, the sRNA sequencing was done to characterize the miRNAs and verify their expression profiles in both the BYC2 and GYC2. In fact, 22 million or more clean reads were obtained from the four libraries. The sRNAs in the toon

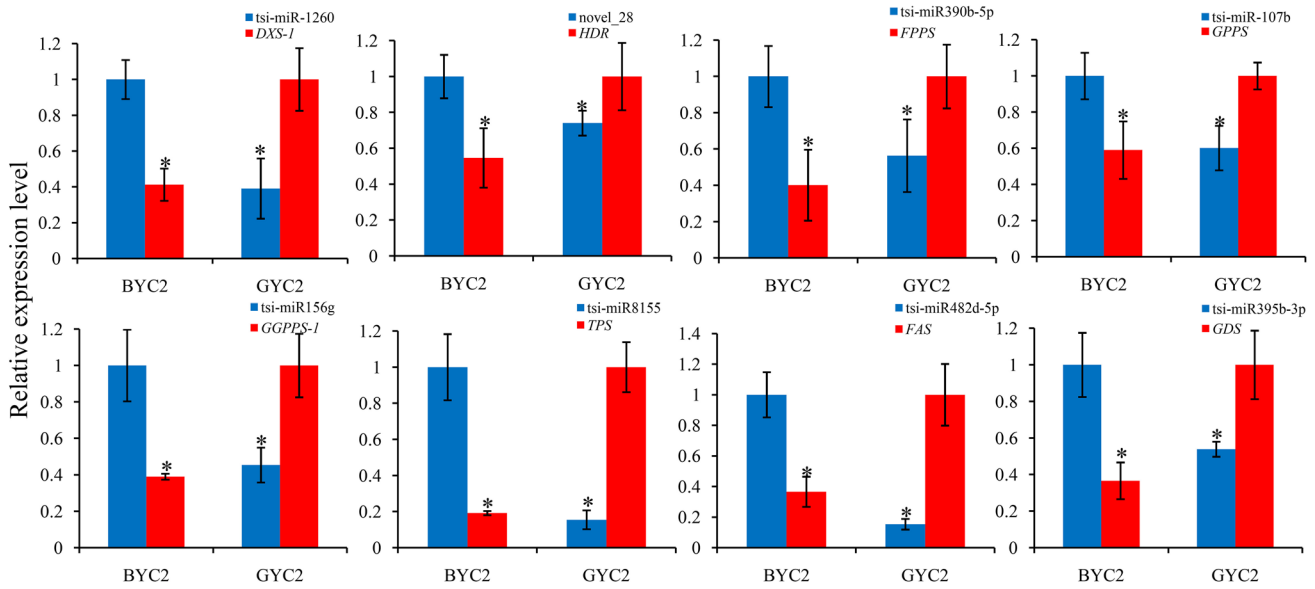

Fig. 7 The qRT-PCR validation of the miRNAs and their target unigenes related to the biosynthesis of volatile terpenoids in BYC2 and GYC2. All the values represent an average ± SD ($n = 6$). The error bars with asterisks are the statistically significant differences (*$P < 0.05$; Student's t test)

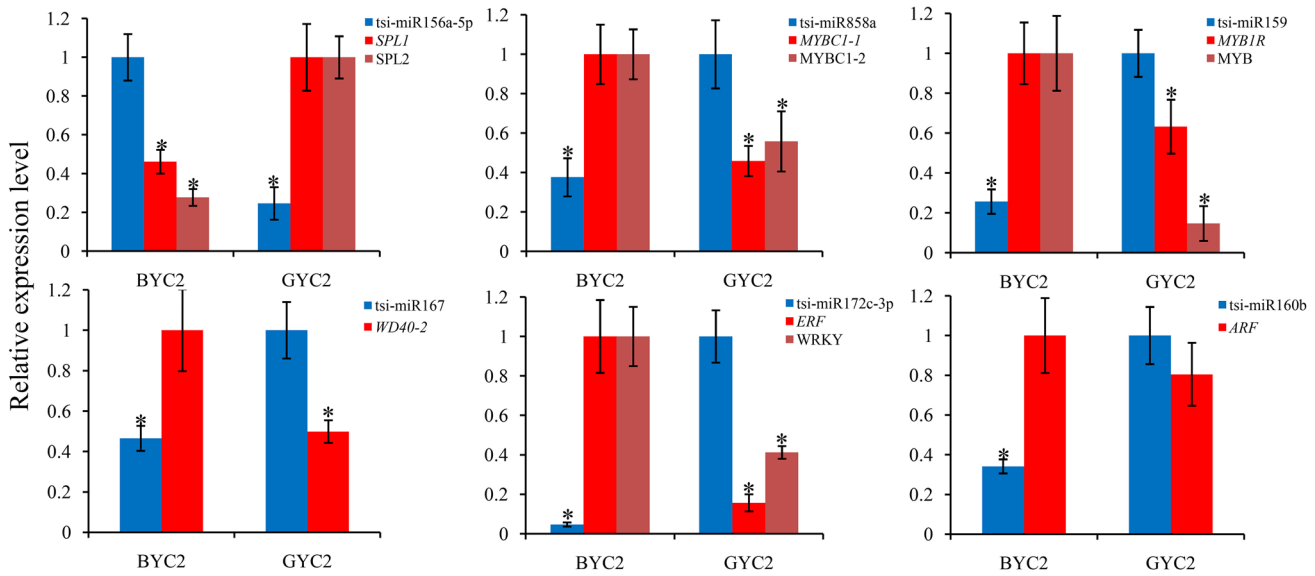

Fig. 8 The qRT-PCR validation of the miRNAs and their transcription factor-associated target unigenes in BYC2 and GYC2. All the values represent an average ± SD ($n = 6$). The error bars with asterisks are the statistically significant differences (*$P < 0.05$; Student's t test)

sprouts exhibited a wide range of variations in length, with the 21-nt RNAs being the most abundant type, followed by 24-nt and 22-nt sRNAs, representing the typical length of the Dicer-cleaved mature plant miRNAs (Moro et al. 2018). Such a distribution pattern of the sRNAs according to length, was also recorded for *Moringa oleifera*, *Solanum tuberosum*, and *Glycine max* (Li et al. 2015; Pirro et al. 2016; Qiao et al. 2017), implying that most miRNAs in the toon sprouts chiefly mediated the cleavage of the target genes, as well as the post-transcriptional inhibition and chromatin modeling of target genes (Axtell 2013; Lee and Carroll. 2018). Among the four sRNA libraries, a total of 331 known miRNAs classified under 56 families and 23 novel miRNAs were identified in the BYC2 and GYC2. Most of the known miRNAs of the toon sprouts exhibited a high degree of sequence conservation with the other plants

in the miRBase database and a comparatively higher read number. Among the miRNAs of the toon sprouts identified, 44 known miRNAs and 8 novel miRNAs were statistically calculated as DE-miRNAs between the BYC2 and GYC2. This implied that these DE-miRNAs may be variety-specific and play crucial roles in the phenotypic determination of the two varieties. Furthermore, the majority of the plant miRNAs possessed almost perfect matches to their targets (Jones-Rhoades et al. 2006). This feature facilitated the identification of their potential targets in the toon sprout. At the same time, it could also provide certain vital information about their putative functions. In our analysis of the target unigenes, a substantial number of potential targets were aligned to the previous transcriptome data. A single miRNA has multiple target genes, whereas a target gene may be recognized and regulated by multiple miRNAs (Wei et al. 2015; Licursi et al. 2019). Further studies focusing on the miRNA-mediated the regulation of the flavonoid and terpenoid pathways are mandatory to elucidate difference in the abundance of the secondary metabolites between the BYC2 and GYC2 varieties. Several miRNAs were bioinformatically predicted to target the unigenes in the biosynthesis pathway of the flavonoid, including *PAL*, *C4H*, *4CL*, *CHS*, *DFR*, and *UGT*, etc. A high expression level of miRNA that targets the genes related to flavonoid formation may inhibits the total flavonoid accumulation. For both the BYC2 and GYC2, the expression levels of the tsi-miR4995, tsi-miR403-3p, novel_27, tsi-miR171c-5p, novel_34, tsi-miR172c, tsi-miR319i, tsi-miR408d, and tsi-miR396b were inversely correlated with the total flavonoid content. The key enzyme genes involved in the flavonoid biosynthetic pathway that were targeted by the miRNAs were previously recorded in *Podophyllum hexandrum*, such as the *4CL* and *CHS* targeted by the phe-miR172i and phe-miR829.1, respectively (Biswas et al. 2016). A similar study was reported in both genotypes of soybean, gma-miR396 and gma-miR5434, which demonstrated an inverse relationship with their corresponding targets *UGT* and *CHI* (chalcone isomerase), respectively (Gupta et al. 2019). The flavor of toon sprouts consists of diverse volatile terpenoid compounds, which were biosynthesized separately in two distinct pathways, the MVA and MEP, respectively. From the target prediction, a total of 13 miRNA-target pairs were identified, that seemed to be directly relevant to the biosynthesis of these terpenoids (Table 5). Among these miRNAs, the expression levels of 8 miRNAs were negatively correlated with the terpenoid contents in the BYC2 and GYC2. For instance, *DXS-1* targeted for tsi-miR-1260 and *HDR* targeted for novel_28 in the MEP pathway, and *FPPS* targeted for the tsi-miR390b-5p, *GPPS* targeted for tsi-miR-107b, *GGPPS* -1 targeted for the tsi-miR156g, *FAS* targeted for the tsi-miR8155, *TPS* targeted for the tsi-miR482d-5p, and *GDS* targeted for the tsi-miR395b-3p in the downstream pathway of the terpenoid biosynthesis. These results indicated that compared with the BYC2, the high abundance of volatile terpenoid in GYC2 was due to the relatively lower levels of expression of these miRNAs. Samad discovered that *DXS* and *DXR* were targeted by pmi-miR396a and pmi-miR398f/g in the MEP pathway, respectively (Samad et al. 2019). However, in our study, these genes were targeted by the *T. sinensis*-specific miRNAs that were different from the reports cited above. A plausible reason is that, in different species, different miRNAs were applied to regulate their targets.

More importantly, the target prediction in this study revealed that certain miRNAs not only targeted the enzyme genes related to the metabolic pathways, they also negatively regulated several transcription factors (TFs). These TFs play a crucial regulatory role in plant growth, development and biosynthesis of secondary metabolites. For example, four *MYB* unigenes were also targeted by ath-miR858a and aqc-miR159. A similar study showed that ath-miR858a targeted the *R2R3-MYB* involved in the biosynthesis of flavonoid in *Arabidopsis thaliana*, and the overexpression of miR858a in transgenic *Arabidopsis* resulted in the down-regulation of several *MYBs* and inhibition of the flavonoid biosynthesis (Sharma et al. 2016). A decrease in the miR858 activity resulted in flavonoid accumulation in the *Arabidopsis* leaves and enhanced its resistance to pathogen infection (Camargo-Ramírez et al. 2018). The WD40 protein was reported to be an essential component of the MYB-bHLH-WD40 (MBW) transcription complex for anthocyanin biosynthesis (Sunitha et al. 2019). The *WD40* transcripts, as potential targets of tsi-miR167 showed higher expression in the BYC2 than in the GYC2. The MBW complex could regulate the *DFR* and *UFGT* expressions to control the anthocyanin biosynthesis in *Arabidopsis* (Xu et al. 2014; Yang et al. 2018). The SPLs are the other TFs widely prevalent in plants, which play an important role in plant growth and development, primary and secondary metabolism (Gou et al. 2012; Yu et al. 2012). In *Arabidopsis*, the pattern of flavonoid or anthocyanin accumulation was under the regulation of miR156-targeted *SPL* gene. The SPLs acted as the negative regulators of anthocyanin accumulation by destabilizing the MBW complex (Gou et al. 2012). On the other hand, the SPLs could directly bind to the *TPS* promoters to act as positive regulators of the biosynthesis of volatile terpenoids (Yu et al. 2015). In our study, the results of the sRNA sequencing and qRT-PCR showed that the tsi-miR156a-5p significantly up-regulated, whereas the expression of its targets *SPLs* were down-regulated in the BYC2 compared to that in the GYC2, which was in accordance with the *TPS* expression level and content of volatile terpenoid as stated above. The tsi-miR172c-3p and tsi-miR160b possibly targeted the *ERF*, *WRKY* and *ARF* TFs to play crucial roles in sucrose signaling. The miR172 and miR160 might target the *ERF* and *ARF* to activate

auxin-mediated signaling (Gao et al. 2019; He et al. 2019). All of these signal transduction processes would induce a profound impact on the activities of the structural genes, and subsequently construct a complex molecular network mechanism to regulate secondary metabolites biosynthesis in the toon sprouts.

Supplementary Information The online version contains supplementary material available at https://doi.org/10.1007/s12374-021-09321-6.

Acknowledgements We would like to thank Dr. Gopal Patel's help to revise the manuscript from Laboratory of Medicinal Plant Biotechnology, Pharmacy College, Zhejiang Chinese Medicine University. We are also grateful to Postgraduate San Peng Fan, Dawei You, and Man Xu for their help to improve the experiment operation from Laboratory of Medicinal Plant Biotechnology, Pharmacy College, Zhejiang Chinese Medicine University. We thank Novogene Technologies (Beijing, China) for supplying small RNA sequencing service.

Author contributions HZ, WZ, and GK conceived and designed this experiment. HZ drafted the manuscript. WL and CQ collected samples of toon sprouts. YC and SF extracted and assayed flavonoid components and volatile terpenoid compounds. PG, HZ and WZ carried out qRT-PCR experiments and analyzed the data. All authors read and approved the manuscript.

Funding This work was supported by grants from the Natural Science Key Foundations of the Anhui Bureau of Education and institution of higher education outstanding top talent cultivation funding project of the Anhui Bureau of Education (No. KJ2019A0515, gxgwfx2020049), the Natural Science Key Foundation of Fuyang normal university (No. 2020FSKJ01ZD), the Innovation Program for College Students (No. 202010371013), the Open Fund of Advantaged and Characteristic Disciplines (Traditional Chinese Medicine of Zhejiang Chinese Medical University) for Key Construction Universities in Zhejiang Province (No. ZYAOX2018027).

Declarations

Conflict of interest The authors declare no conflict of interest.

References

Audic S, Claverie JM (1997) The significance of digital gene expression profiles. Genome Res 7:986–995

Axtell MJ (2013) Classification and comparison of small RNAs from plants. Annu Rev Plant Biol 64:137–159

Axtell MJ, Meyers BC (2018) Revisiting criteria for plant microRNA annotation in the era of big data. Plant Cell 30:272–284

Baggerly KA, Deng L, Morris JS, Aldaz CM (2003) Differential expression in SAGE: accounting for normal between-library variation. Bioinformatics 19:1477–1483

Biswas S, Hazra S, Chattopadhyay S (2016) Identification of conserved miRNAs and their putative target genes in *Podophyllum hexandrum* (Himalayan Mayapple). Plant Gene 6:82–89

Bulgakov VP, Avramenko TV (2015) New opportunities for the regulation of secondary metabolism in plants: focus on microRNAs. Biotechnol Lett 37:1719–1727

Camargo-Ramírez R, Val-Torregrosa B, Segundo BS (2018) MiR858-mediated regulation of flavonoid-specific MYB transcription factor genes controls resistance to pathogen infection in *Arabidopsis*. Plant Cell Physiol 59:190–204

Chen QQ, Rong LY, Shao ZJ, Liu T, Wei L, Song ZQ (2018) Genetic diversity analysis of *Toona sinensis* germplasms based on SRAP and EST-SSR markers. Acta Hortic Sinica 45:967–976

Chen YC, Chen HJ, Huang BM, Chen YC, Chang CF (2019) Polyphenol-rich extracts from *Toona sinensis* bark and fruit ameliorate free fatty acid-induced lipogenesis through AMPK and LC3 pathways. J Clin Med 8:1664

Edmonds JM, Staniforth M (1998) *Toona Sinensis*: Meliaceae. Curtis's Bot Mag 15:186–193

Fan R, Li Y, Li C, Zhang Y (2015) Differential microRNA analysis of glandular trichomes and young leaves in *Xanthium strumarium* L. reveals their putative roles in regulating terpenoid biosynthesis. PLoS ONE 10:e0139002

Friedlander MR, Mackowiak SD, Li N, Chen W, Rajewsky N (2011) miRDeep2 accurately identifies known and hundreds of novel microRNA genes in seven animal clades. Nucleic Acids Res 40:37–52

Gao J, Peng H, Chen FB, Luo M, Li WB (2019) Genome-wide analysis of transcription factors related to anthocyanin biosynthesis in carmine radish (*Raphanus sativus L.*) fleshy roots. Peer J 7:e8041

Gou JY, Felippes FF, Liu CJ, Weigel D, Wang JW (2012) Negative regulation of anthocyanin biosynthesis in *Arabidopsis* by a miR156-targeted SPL transcription factor. Plant Cell 23:1512–1522

Gupta OP, Dahuja A, Sachdev A, Kumari S, Jain PK, Vinutha T, Praveen S (2019) Conserved miRNAs modulate the expression of potential transcription factors of isoflavonoid biosynthetic pathway in soybean seeds. Mol Biol Rep 46:3713–3730

He LH, Tang RM, Shi XW, Wang WB, Cao QH, Liu XY, Wang T, Sun Y, Zhang HM, Li RZ, Jia XY (2019) Uncovering anthocyanin biosynthesis related microRNAs and their target genes by small RNA and degradome sequencing in tuberous roots of sweet potato. BMC Plant Biol 19:232

Hsu CY, Huang PL, Chen CM, Mao CT, Chaw SM (2012) Tangy scent in *Toona sinensis* (Meliaceae) leaflets: isolation, functional characterization, and regulation of *TsTPS1* and *TsTPS2*, two key terpene synthase genes in the biosynthesis of the scent compound. Curr Pharm Biotechnol 13:1–12

Jiang XX, Zhang BB, Lei MH, Zhang JJ, Zhang JF (2019) Analysis of nutrient composition and antioxidant characteristics in the tender shoots of Chinese toon picked under different conditions. LWT-Food Sci Technol 109:137–144

Jones-Rhoades MW, Bartel DP, Bartel B (2006) MicroRNAs and their regulatory roles in plants. Annu Rev Plant Biol 57:19–53

Kanehisa M, Furumichi M, Tanabe M, Sato Y, Morishima K (2017) KEGG: new perspectives on genomes, pathways, diseases and drugs. Nucleic Acids Res 45(D1):D353–D361

Langmead B, Trapnell C, Pop M, Salzberg SL (2009) Ultrafast and memory-efficient alignment of short DNA sequences to the human genome. Genome Biol 10:R25

Lee CH, Carroll BJ (2018) Evolution and diversification of small RNA pathways in flowering plants. Plant Cell Physiol 59:2169–2187

Li WB, Wang PP, Li YG, Zhang KX, Ding FQ, Nie TK, Yang X, Lv QX, Zhao L (2015) Identification of microRNAs in response to different day lengths in soybean using high-throughput sequencing and qRT-PCR. PLoS ONE 10:e0132621

Licursi V, Conte F, Fiscon G, Paci P (2019) MIENTURNET: an interactive web tool for microRNA-target enrichment and network-based analysis. BMC Bioinform- 20:545

Liu BB, Zhang JF, Shi YC (2019) Complete chloroplast genome of *Toona sinensis* (Meliaceae), a goluptious 'tree vegetables.' Mitochondrial DNA Part B 4:3025–3026

Meyers BC, Axtell MJ, Bartel B, Bartel DP, Baulcombe D, Bowman JL, Cao XF, Carrington JC, Chen XM, Green PJ, Griffiths-Jones S, Jacobsen SE, Mallory AC, Martienssen RA, Poethig RS, Qi YJ, Vauchere H, Voinnet O, Watanabe Y, Weigel D, Zhu JK (2008) Criteria for annotation of plant microRNAs. Plant Cell 20:3186–3190

Moro B, Chorostecki U, Arikit S, Suarez IP, Höbartner C, Rasia RM, Meyers BC, Palatnik JF (2018) Efficiency and precision of microRNA biogenesis modes in plants. Nucleic Acids Res 46:10709–10723

Peng W, Liu YJ, Hu MB, Zhang MM, Yang J, Liang F, Huang QW, Wu CJ (2019) *Toona sinensis*: A comprehensive review on its traditional usages, phytochemisty, pharmacology and toxicology. Rev Bras Farmacogn 29:111–124

Pirro S, Zanella L, Kenzo M, Montesano C, Minutolo A, Potesta M, Sobze MS, Canini A, Cirilli M, Muleo R, Colizzi V, Galgani A (2016) MicroRNA from *Moringa oleifera*: identification by high throughput sequencing and their potential contribution to plant medicinal value. PLoS ONE 11:e0149495

Prakash P, Ghosliya D, Gupta V (2015) Identification of conserved and novel microRNAs in Catharanthus roseus by deep sequencing and computational prediction of their potential targets. Gene 554:181–195

Prakash P, Rajakani R, Gupta V (2016) Transcriptome-wide identification of *Rauvolfia serpentina* microRNAs and prediction of their potential targets. Comput Biol Chem 61:62–74

Qiao Y, Zhang JJ, Zhang JW, Wang ZW, Ran A, Guo HX, Wang D, Zhang JL (2017) Integrated RNA-seq and sRNA-seq analysis reveals miRNA effects on secondary metabolism in *Solanum tuberosum* L. Mol Genet Genomics 292:37–52

Rogers K, Chen XM (2013) Biogenesis, turnover, and mode of action of plant microRNAs. Plant Cell 25:2383–2399

Samad AFA, Sajad M, Nazaruddin N, Fauzi IA, Murad AMA, Zainal Z, Ismail I (2017) MicroRNA and transcription factor: key players in plant regulatory network. Front Plant Sci 8:565

Samad AFA, Rahnamaie-Tajadod R, Sajad M, Jani J, Murad AMA, Noor NM, Ismail I (2019) Regulation of terpenoid biosynthesis by miRNA in *Persicaria minor* induced by *Fusarium oxysporum*. BMC Genomics 20:586

Sharma D, Tiwari M, Pandey A, Bhatia C, Sharma A, Trivedi PK (2016) MicroRNA858 is a potential regulator of phenylpropanoid pathway and plant development. Plant Physiol 171:944–959

Shen YP, Xu MH, Deng PP, Gu QY, Yin HW, Xia GH, Jia XB, Yang H, Tam J (2017) Establishment of a rapid method to quantify eight flavonol glycosides for quality assessment of red toon using UPLC. Acta Chromatogr 30:1–7

Singh N, Srivastava S, Sharma A (2016) Identification and analysis of miRNAs and their targets in ginger using bioinformatics approach. Gene 575:570–576

Singh A, Gautam VS, Das SS, Verma S, Mishra V, Mukherjee S, Sarkar AK (2018) Plant small RNAs: advancement in the understanding of biogenesis and role in plant development. Planta 248:545–558

Sui JJ, Qu CQ, Yang JX, Zhang WN, Ji YT (2019) Transcriptome changes in the phenylpropanoid pathway in senescing leaves of *Toona sinensis*. Acta Physiol Plant 41:126

Sun YY, Qiu Y, Duan MM, Wang JL, Zhang XH, Wang HP, Song JP, Li XX (2017) Identification of anthocyanin biosynthesis related microRNAs in a distinctive Chinese radish (*Raphanus sativus* L.) by high-throughput sequencing. Mol Genet Genomics 292:215–229

Sunitha S, Loyola R, Alcalde JA, Arce-Johnson P, Matus JT, Rock CD (2019) The role of UV-B light on small RNA activity during grapevine berry development. G3 9:769–787

Vashisht I, Mishra P, Pal T, Chanumolu S, Singh TR, Chauhan RS (2015) Mining NGS transcriptomes for miRNAs and dissecting their role in regulating growth, development, and secondary metabolites production in different organs of a medicinal herb, *Picrorhiza kurroa*. Planta 241:1255–1268

Wei RC, Qiu DY, Wilson IW, Zhao H, Lu SF, Miao JH, Feng SX, Bai LH, Wu QH, Tu DP, Ma XJ, Tang Q (2015) Identification of novel and conserved microRNAs in *Panax notoginseng* roots by high-throughput sequencing. BMC Genomics 16:835

Wen M, Shen Y, Shi S, Tang T (2012) miREvo: an integrative microRNA evolutionary analysis platform for next-generation sequencing experiments. BMC Bioinformatics 13:140

Wu HJ, Ma YK, Chen T, Wang M, Wang XJ (2012) PsRobot: a web-based plant small RNA meta-analysis toolbox. Nucleic Acids Res 40:W22–W28

Xia R, Zhu H, An YQ, Beers EP, Liu ZR (2012) Apple miRNAs and tasiRNAs with novel regulatory networks. Genome Biol 13:R47

Xu WJ, Grain D, Bobet S, Gourrierec JL, Thévenin J, Kelemen Z, Lepiniec L, Dubos C (2014) Complexity and robustness of the flavonoid transcriptional regulatory network revealed by comprehensive analyses of MYB–bHLH–WDR complexes and their targets in *Arabidopsis* seed. New Phytol 202:132–144

Xu XB, Jiang QH, Ma XY, Ying QC, Shen B, Qian YS, Song HM, Wang HZ (2015) Deep sequencing identifies tissue-specific microRNAs and their target genes involving in the biosynthesis of tanshinones in *Salvia miltiorrhiza*. PLoS ONE 9:e111679

Yang JF, Li BB, Shi WJ, Gong ZZ, Chen L, Hou ZX (2018) Transcriptional activation of anthocyanin biosynthesis in developing fruit of blueberries (*Vaccinium corymbosum* L.) by preharvest and postharvest UV irradiation. J Agric Food Chem 66:10931–10942

Ye J, Zhang Y, Cui HH, Liu JW, Wu YQ, Cheng Y, Xu HX, Huang XX, Li ST, Zhou A, Zhang XQ, Bolund L, Chen Q, Wang J, Yang HM, Fang L, Shi CM (2018) WEGO 2.0: a web tool for analyzing and plotting GO annotations, 2018 update. Nucleic Acids Res 46(W1):W71–W75

Yu S, Galvão VC, Zhang YC, Horrer D, Zhang TQ, Hao YH, Feng YQ, Wang S, Schmid M, Wang JW (2012) Gibberellin regulates the Arabidopsis floral transition through miR156-targeted SQUAMOSA PROMOTER BINDING–LIKE transcription factors. Plant Cell 24:3320–3332

Yu ZX, Wang LJ, Zhao B, Shan CM, Zhang YH, Chen DF, Chen XY (2015) Progressive regulation of sesquiterpene biosynthesis in *Arabidopsis* and Patchouli (*Pogostemon cablin*) by the miR156-targeted SPL transcription factors. Mol Plant 8:98–110

Zhai XT, Granvogl M (2019) Characterization of the key aroma compounds in two differently dried *Toona sinensis* (A. Juss.) Roem. by means of the molecular sensory science concept. J Agric Food Chem 67:9885–9894

Zhang BH, Unver T (2018) A critical and speculative review on microRNA technology in crop improvement: current challenges and future directions. Plant Sci 274:193–200

Zhang X, Song ZQ, Liu T, Guo LL, Li XF (2016) De Novo assembly and comparative transcriptome analysis provide insight into lysine biosynthesis in *Toona sinensis* Roem. Int J Genom 3:1–9

Zhao H, Ren LP, Fan XY, Tang KJ, Li B (2017) Identification of putative flavonoid-biosynthetic genes through transcriptome analysis of Taihe *Toona sinensis* bud. Acta Physiol Plant 39:122

Zhao H, Feng SS, Zhou W, Kai GY (2019) Transcriptomic analysis of postharvest toon buds and key enzymes involved in terpenoid biosynthesis during cold storage. Sci Hortic 257:108747

Zhou L, Chen JH, Li ZZ, Li XX, Hu XD, Huang Y, Zhao XK, Liang CZ, Wang Y, Sun L, Shi M, Xu XH, Shen F, Chen MS, Han ZJ, Peng ZY, Zhai QN, Chen J, Zhang ZF, Yang RL, Ye JX, Guan ZC, Yang HM, Gui YT, Wang J, Cai ZM, Zhang XQ (2010) Integrated profiling of microRNAs and mRNAs: microRNAs located on Xq27.3 associate with clear cell renal cell carcinoma. PLoS ONE 5:e15224